Structural Review of Phase-change Recording Materials for Practical Use

Toshiyuki Matsunaga [a], Rie Kojima [b], Noboru Yamada [b], Kouichi Kifune [c], Yoshiki Kubota[d], Sinji Kohara [e]

[a] Material&Process Development Center, Panasonic Corporation
3-1-1 Yagumo-Nakamachi, Moriguchi, Osaka 570-8501, Japan
Correspondence e-mail: matsunaga.toshiyuki@jp.panasonic.com

[b] Advanced Technology Research Laboratories, Panasonic Corporation
[c] Faculty of Liberal Arts and Sciences, Osaka Prefecture University
[d] Graduate School of Science, Osaka Prefecture University
[e] Japan Synchrotron Radiation Research Institute/SPring-8

ABSTRACT

Phase change recording is now extensively used for high density non-volatile memories. The typical phase-change materials are GeTe-Sb_2Te_3 pseudo-binary alloys and Sb-Te based multinary alloys with some dopants such as Ag-In-Sb-Te quadruple compounds. These crystals approximately have two kinds of crystalline, metastable and stable phases. The crystals of these metastable phases are rather simple and can be approximated by cubic structures; on the other hand, those of stable phases have very complicated long-period layered structures. The crystal structures of these two phase-change recording materials surprisingly resemble each other; all these crystals have 3+3 coordination structures in average. However, the atomic configuration in the GST materials abruptly changes with temperature from the metastable phase to the stable phase at first-order phase transition; on the other hand, it continuously varies in the AIST materials. Such 3+3 coordination structures are found also in amorphous AIST, the atoms in amorphous GST also have three coordination atoms in numeric average. It is an interesting idea that this coordination structure feature is held also in both their crystalline phases; in other words, it is kept during whole phase transformation.

Key words: phase-change memory, GST, AIST, XRD, structural analysis, Rietveld method

1. INTRODUCTION

Phase change recording is now extensively used for high density non-volatile memories [1]. Since 1970s, various materials have been proposed for the purpose, and today we have obtained two superior materials of GeTe-Sb_2Te_3 (GST) [2] and Sb-Te based alloys such as Ag-In-Sb-Te quadruple compounds (AIST) [3]. The crystal structures of these materials are astonishingly similar to each other. Their stable phases are long-period stacking structures with cubic close-packed periodicity, and they obtain these stable structures through simple six-layer structures from their amorphous phases: GST materials show NaCl-type average structures just after the phase transformation; on the other hand AISTs exhibit A7-type structures as transient structures. These two kinds of transient structures are very similar to each other as well as the stable structures; furthermore, all these transient and stable crystals can be described as commensurately or incommensurately modulated structures. As for the amorphous phases, their structures are also similar to each other; because they consist of molecules formed by covalently bonded group-IV, V, or IV atoms. In these amorphous phases, the atoms have three nearest neighbors in average. This coordination structure feature is held also in their crystalline phases. In this paper, crystal structures of these two kinds of materials are described in detail comparing with each other, and then, structural transformations in the crystalline phases are shown in detail. We will see that structural transformation from the amorphous phase to the stable crystalline phase is acquisition of anisotropic and long-range periodicities keeping the 3+3 coordination structures.

2. EXPERIMENTS

The phase-change recording cholcogenide thin films shown in this paper were formed by sputtering on glass disks 120

mm in diameter. Their thicknesses were approximately 300 nm. The films were scraped off with a spatula to create powder specimens, and they were packed into quartz capillary tubes with internal diameters of 0.2 - 0.3 mm for X-ray diffraction measurements. The openings of the capillaries were sealed by using an oxyacetylene flame to insulate them against the atmosphere. The diffraction experiments were carried out using the large-diameter Debye-Scherrer camera with an imaging plate on the BL02B2 beam line at SPring-8 [4]. In order to confirm the radiation beam energy used, diffraction pattern of powdered CeO_2 (a = 5.4111 Å) was taken under the same conditions. The experiments at low and high temperatures were carried out while blowing nitrogen gas set at the specified temperatures onto the capillary tubes. The crystal structures were examined and refined using the Rietveld method [5]. The program JANA2000 [6] was used for this purpose; intensity data in increments of 0.01° were obtained by reading the imaging plate for a pixel area of 50 μm^2.

3. RESULTS & DISCUSSION

3-1) stable homologous structures

Two kinds of chalcogenide compunds, GeTe-Sb_2Te_3 and Sb-Te, are now extensively used for phase change memory materials (Sb-Te materials are used by adding some other elements such as Ag or In as dopants to stabilize their amorphous phases and to facilitate the recrystallization). It has been found that in thermal equilibrium, these systems form various intermetallic compounds represented by the chemical formulas $(GeTe)_n(Sb_2Te_3)_m$ and $(Sb_2)_n(Sb_2Te_3)_m$ (n, m: integer), respectively. All these compounds have trigonal structures with $2n + 5m$ cubic close-packed periodicity without exception (more specifically, the residual of $(2n + 5m)/3 = 0$ and $\neq 0$ leads to the formation of crystals having structures with primitive (P) and rhombohedral (R) unit cells, respectively); and they are called homologous compounds because of their similarity in structure. These two kinds of (pseudo-) binary crystals are isostructures to each other when n and m each are the same as those of the other. Their structures are systematically characterized by the stacking of the $(GeTe)_n$ and $(Sb_2Te_3)_m$ or $(Sb_2)_n$ and $(Sb_2Te_3)_m$ blocks along the c_H-axes, with very long cell dimensions in the conventional three-dimensional (3-D) structure description [7-16]. More generally and more precisely, it has been assumed that these structures should be described as commensurately or incommensurately modulated four-dimensional (4-D) structures characterized by modulation vectors $\boldsymbol{q} = \gamma \cdot \boldsymbol{c}^*_{sub}$ [17] (As seen in Fig. 1; $\boldsymbol{c}^*_{sub}$ is the fundamental reciprocal vector formed by three-layer cubic stacking). If these compounds form incommensurately modulated structures we can simply derive γ in terms of x as

$$\gamma = 2 - x/2, \qquad (1)$$

when the chemical formula for these (pseudo-)binary systems are written as $(GeTe)_x(Sb_2Te_3)_{1-x}$, or Sb_xTe_{1-x} [17]; on the other hand, when they form commensurately modulated structures, γs are restricted to (discrete) rational numbers written by $3(n + 3m)/(2n + 5m)$. In the GeTe-Sb_2Te_3 pseudo-binary system, several intermetallic compounds exclusively crystallized into commensurately modulated structures, $Ge_3Sb_2Te_6$ (n=3, m=1; 11R)[13], $Ge_2Sb_2Te_5$ (n=2, m=1; 9P)[12], $Ge_1Sb_2Te_4$ (n=1, m=1; 7R)[11],

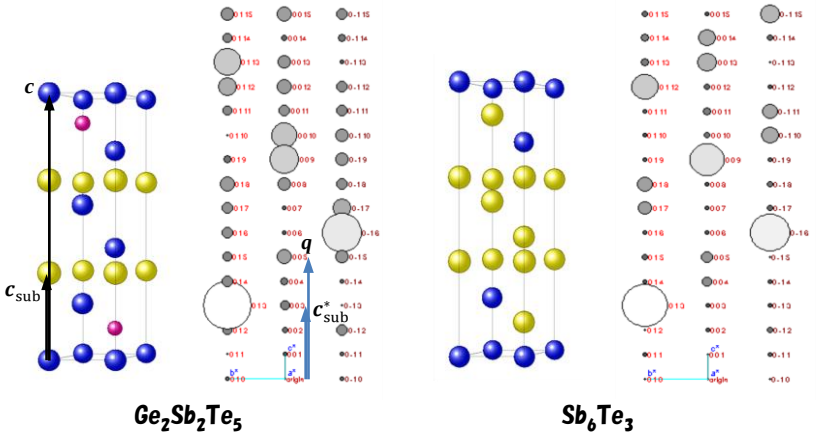

Fig. 1. The crystal structures of $Ge_2Sb_2Te_5$ and Sb_6Te_3 and their diffraction patterns. The structures are shown in perspective, in which Ge, Sb, and Te are indicated by purple, yellow and blue, respectively. The $0k\ell$ diffraction planes are depicted in a square range of $-1 \le k \le 1$ and $0 \le \ell \le 15$. The diameters of the reciprocal points in the patterns are in proportion to the absolute values of their structure factors $F(hk\ell)$. The atomic layers along the c_H-axis are arranged by two kinds of vectors in these structures: one is the fundamental reciprocal vector formed by three-layer cubic stacking and the other is a modulation vector expressed by $\boldsymbol{q} = \gamma \cdot \boldsymbol{c}^*_{sub}$. The former vector gives fundamental reflections; on the other hand, the latter produces superstructure reflections in the diffraction patterns. The γ value of these crystals is a rational number 5/3; which means that they are both commensurate structures. In actual $Ge_2Sb_2Te_5$ crystals, it is presumed that the Ge and Sb sites are partially substituted by Sb and Ge atoms, respectively [12].

$Ge_1Sb_4Te_7$ (n=1, m=2; 12P)[15], and $Ge_1Sb_6Te_{10}$ (n=1, m=3; 17R)[16], have been found up to now to our knowledge; while it has been presumed that the Sb-Te binary system contains not only such intermetallic compounds as the GST materials but also a (wide) composition region seamlessly filled with incommensurate Sb_xTe_{1-x} compounds around Sb:Te=1:1. The crystal structures of $Ge_2Sb_2Te_5$ and Sb_6Te_3 are shown in Fig. 1 to aid in the understanding of these calcogenide structures; we can observe in these structural models that these compounds have isostructures to each other. The γ value of these crystals is 5/3, which means that both the compounds have commensurately modulated structures. In these structures, all the constituent atoms have 3+3 coordination atoms, which form distorted octahedral coordination. The central atom is more strongly bonded with the shorter three atoms than the other three. It is very interesting and highly suggestive that these two kinds of materials crystallize into isostructures in the thermal equilibrium. However, in GST intermetallic compounds discretely appear compared with Sb-Te compounds. This is presumed to be due to the fact that Ge atoms always occupy the $\bar{3}m$ sites of their space groups, $P\bar{3}m1$ and $R\bar{3}m$. These compounds generally hold material properties of narrow band gap semiconductors and low thermal conductivities; presumably, these calcogenide materials and their composites are not only used as phase-change recording materials but also expected to be used for elements in thermoelectric devices.

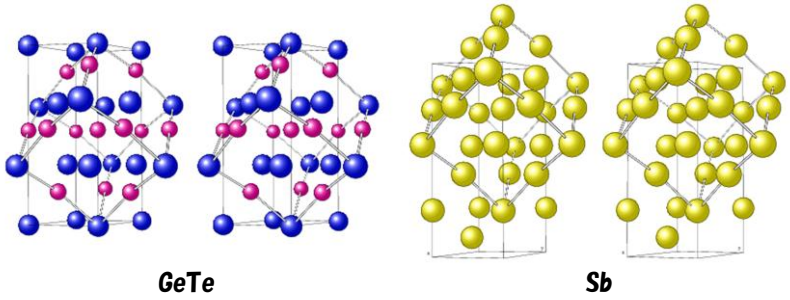

Fig. 2. The structures of the GeTe low-temperature phase ($R3m$) and Sb ($R\bar{3}m$) shown in the hexagonal (thin lines) unit cells. The NaCl-type structure of the high-temperature phase for GeTe drawn with thick lines is deformed by the phase transition to the low-temperature phase. (pseudo-)cubic cell is depicted with thick lines as well also in the Sb structure model. This large cubic cell is composed of eight small, pseudo simple cubic cells. As seen in these drawings, both crystals are six-layer structures and any constituent atom has six (3+3) coordination atoms (three atoms at upper layer + three atoms at lower layer). These stereographic drawings are set up for parallel-viewing.

3-2) metastable transient structures

Just after the phase transformation from the amorphous phase, which corresponds to deleting recorded marks in optical disks, GST and AIST amorphous compounds both crystallize into six-layer homologous structures. The formers are B1-type (NaCl) structures; on the other hand, the latters are A7-type (α-As) structures. The A7-type crystals hold 3+3 coordination structures as well as other homologous crystals mentioned above. The octahedra formed by these coordination atoms are oriented along the c-axis direction. Recently, it has been found that GeTe also maintains 3+3 coordination structure even in its high-temperature cubic phase; however, the octahedra of this crystal are randomly distributed different from the case of AIST [18] (Not only in this binary compound but also in GST pseudo-binary cubic compounds, we believe that such coordination structures remains even in their cubic phases). These two structures are naturally very similar to each other as seen in Fig. 2, because they are ones of homologous structures in common. If Ge and Te atoms are randomly located at any atomic sites of the GeTe crystal, its structure coincides with that of Sb. These structures are the simplest (γ=3/2) of all the homologous structures crystallized at the shortest layer period, and they are spatially isotropic, which can be well approximated by cubic structures. We have been asserting that the materials that can take such simple and spatially isotropic structures just after the recrystallization are suitable for high-speed phase-change recording materials; it is presumed that such a structural property is one of essential features for them because topological resemblance is required for reduction of atomic switch lengths through the phase change.

3-3) structural transformations in the crystalline phases

As mentioned in the introduction, NaCl-type GST (metastable) crystals transform to the stable trigonal structures by giving sufficient heat treatments. These structural transformations are first-order phase transition phenomena. The former crystals suddenly change to the latters when raising the temperature. These transition temperatures have been examined by the differential scanning calorimetry [2]. For instance, metastable $Ge_2Sb_2Te_5$ maintains its NaCl-type

structure up to 230 ºC; above this transition temperature the crystal abruptly changes to 9-layer trigonal structure (see Fig. 1) with showing an exothermic peak. The γ values characterizing these structures are 3/2 and 5/3, respectively; the above means that γ discretely changes from the former to the latter at its specific transition temperature. In the cases of $Ge_1Sb_2Te_4$, it falls into 21-layer structure (γ=12/7) at 210 ºC. The metastable compounds with NaCl-type simple structures appear over a wide composition range of GeTe from 100 mol% to at least 33.3 mol%; however, it has been found that the transition temperature gradually rises with increasing GeTe content, which means that the NaCl-type metastable phase conversely becomes unstable with increased Sb_2Te_3. At 100% GeTe of the pseudo-binary line, NaCl-type GeTe itself is the stable phase; on the other hand, we have hardly observed $Ge_1Sb_6Te_{10}$ (25 mol% GeTe) compounds crystallized into an NaCl-type structure. Different from these GST compounds, however, the atomic rearrangements in Sb-Te crystals show second order-like phase transformations.

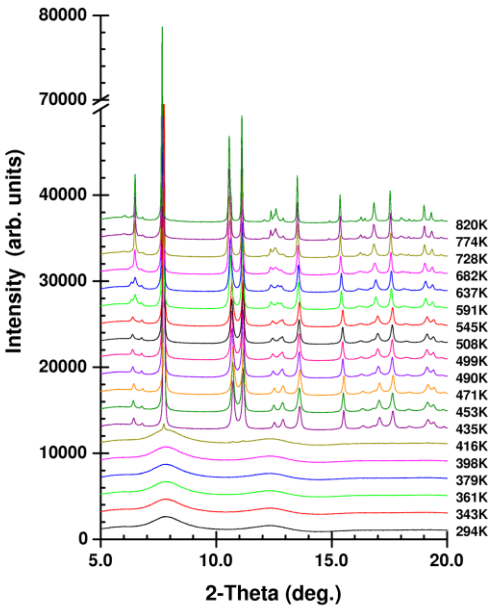

Fig. 3. Temperature dependence of the X-ray powder diffraction profiles for a sputtered $Ag_{3.4}In_{3.7}Sb_{76.4}Te_{16.5}$ amorphous film in a heating process. The amorphous halo patterns are observed at low temperatures from 295 K to 416 K; however at around 416 K, the Bragg peaks of A7-type structure appear in the halo pattern. As temperature is raised further, the A7-type single phase separates into two phases, $AgInTe_2$ and an Sb-Te binary compound, at around 591 K. At lower 2θ angles than 5º, Bragg peaks were hardly observed at any measurement temperatures.

Sb-Te materials are used in practice as phase-change recording materials by doping third and/or fourth elements such as Ag and/or In to improve the endurance of the amorphous phases and raise the phase-change speed to the crystalline phase. As has mentioned above, this quadruple material is called AIST. The diffraction patterns in heating process obtained for the sputtered AIST ($Ag_{3.4}In_{3.7}Sb_{76.4}Te_{16.5}$) amorphous film are shown in Fig. 3. The amorphous phase transformed into an A7-type crystalline single phase, as seen in this graph, at around 416 K. This six-layer crystalline phase is kept up to around 545 K; however, phase separation written by the following equation takes place above this temperature.

$$Ag_{3.4}In_{3.7}Sb_{76.4}Te_{16.5} \rightarrow Ag_{3.4}In_{3.4}Te_{6.8} + In_{0.3}Sb_{76.4}Te_{9.7}. \quad (2)$$

The first decomposition product has a $CuFeS_2$-type structure, which was tightly held up to the melting temperature around 870 K. The second product, which can virtually be regarded as an Sb-Te binary compound written as $Sb_{89}Te_{11}$ (when expressed as a percentage), gradually changes its atomic arrangement with increasing temperature until obtaining the final stable crystal structure. The results of the Rietveld analysis at 820 K are shown in Table I and Fig. 4. The atomic configuration determined for the latter is shown in Fig. 5. As seen in Fig. 6, γ maintained a constant value of 1.5 up to a temperature of around 591 K, at which $AgInTe_2$ ($CuFeS_2$-type structure) came out. However, above this temperature, γ continuously grew larger with increasing temperature and reached a value of around 1.55 at high temperatures near the melting point of $Sb_{76.4}Te_{9.7}$ (=$Sb_{88.7}Te_{11.3}$ ≈ $Sb_{89}Te_{11}$), which was found at around 870 K according to our present high-temperature measurement. This γ value corresponded well with the value of 1.5565 expected from the composition of $Sb_{88.7}Te_{11.3}$ (see Eq. [1]). Not only the AIST material, non-doped Sb-Te amorphous materials show such continuous changes with temperature as well. For instance, γ of Sb_8Te_3 amorphous sputtered film shows 1.60 just after the crystallization; however, with increasing temperature, it gradually grows to finally obtain its intrinsic structure, i.e., commensurately modulated structure with γ=1.638 [19]. Not only Sb_8Te_3 but also some other various Sb-Te compounds have shown the same behavior [now preparing a paper for submission].

As has so far been shown, the structural transformations with temperature in the two materials are notably different from each other. In the GST pseudo-binary materials, γ abruptly changes with temperature at first-order phase transition; on the other hand, in the Sb-Te binary materials, it continuously varies. The latter variation behaves like a second-order phase transition phenomenon. However, also in these binary compounds, it is presumed that atomic migrations for the structural transformations are realized by passing through between the potential barriers formed by

other atoms; this means that the atomic diffusion with exothermic reaction is locally caused even in the structural transformation of Sb-Te material. As for materials with Ge atoms, on the other hand, it is conceivable that such obvious first-order phase transitions observed on these materials will probably result from simultaneous breaking of sp^3-electronic configurations of Ge atoms at the specific temperatures. As mentioned above, atomic configuration is heavily disordered in the NaCl-type structure of GST material, in which a large number of Ge atoms have 3+3 coordination atoms; this means that they still hold the sp^3-hybridized bonding nature partially even in the crystalline phase. Whereas, on the other hand, Ge atoms in the stable homologous structures are located at the $\bar{3}m$ positions to have six coordination atoms at equidistant without exception, which means that almost all these Ge atoms are in sufficiently isotropic p-p bonding state with their six coordination atoms.

As has so far been shown, an Sb-Te compound containing Ag and In maintains a six-layer structure (γ = 3/2) up to a high temperature, at which phase separation occurs. On the other hand, Sb-Te films without such dopants show γ values larger than 3/2 immediately after the crystallization. This strongly suggests that the Ag and In dopants work on maintaining the A7-type simple structure. It also inversely implies that every Sb-Te binary-compound film will experience a six-layer structure in a very short time right after the crystal formation because this is the simplest and shortest layer structure out of all of the possible homologous structures from Sb (γ = 3/2) to Sb_2Te_3 (γ = 9/5). Many studies (for instance, see Ref. [20]) have shown that phase-change chalcogenide amorphous materials have spatially isotropic atomic arrangements; it is highly likely that they crystallize once into simple and spatially isotropic structures, like a cubic crystal, because a six-layer (A7-type) structure can be well approximated by simple cubic lattices [21].

3-4) basic structure maintained during whole phase transformation

Table I. (a) Final structural parameters determined by 4-D superspace refinements of $Sb_{89}Te_{11}$ and conventional 3-D refinements of $AgInTe_2$ at 820 K. The *R*-factors for the entire pattern ($Sb_{89}Te_{11}$+$AgInTe_2$) are R_p = 1.59% and R_{wp}= 2.21%. The superspace group for $Sb_{89}Te_{11}$ was assumed to be $R\bar{3}m(00g)00$; on the other hand, $I\bar{4}2d$ was applied for $AgInTe_2$. The diffraction data used for the analysis: $5.50° \leq 2\theta \leq 31.30°$. The standard deviations are shown in parentheses. B_n^s represents the positional modulation amplitude, whereas U_s represent the atomic displacement parameters.

$Sb_{89}Te_{11}$:

R-factors of profile and all reflections		
	RF_{obs}	2.16%
	RF_{wobs}	1.29%
R-factors of main and satellite reflections		
Main		
	RF_{obs}	1.48%
	RF_{wobs}	0.78%
R-factors of satellites		
1st order		
	RF_{obs}	3.71%
	RF_{wobs}	3.16%

γ = 1.5527(2); a = 4.3210(1), c = 5.7151(2) Å

atom	*g*	*x*	*y*	*z*	B_1^s	B_2^s	B_3^s	U_{11}(Å^2)	U_{33}(Å^2)
Sb	1.0	0	0	0	0.0284(2)	0.047(1)	0.013(1)	0.0383(1)	-0.008(2)
Te	1.0	0	0	0	0.29(1)	–	–	0.0383	-0.008

$AgInTe_2$:

RF_{obs} = 4.35%, RF_{wobs} = 1.88%, a = 6.4491 (4) Å, and c = 12.612 (1) Å

atom	site	*g*	*x*	*y*	*z*	U_{iso} (Å^2)
Ag	4*b*	1.0	0	0	1/2	0.074
In	4*a*	1.0	0	0	0	0.074
Te	8*d*	1.0	0.25(2)	1/4	1/8	0.074(2)

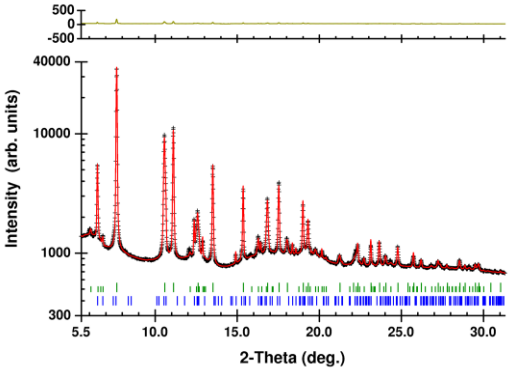

Fig. 4. Observed (+) and calculated (red line) X-ray diffraction profiles for $Ag_{3.4}In_{3.7}Sb_{76.4}Te_{16.5}$ ($AgInTe_2$ + $Sb_{89}Te_{11}$) at 820 K by Rietveld analysis. A difference curve (observed–calculated) appears at the top of the figure; reflection markers are indicated by vertical spikes below the diffraction patterns. Of the spikes at the top, the longer ones are for the fundamental peaks of $Sb_{89}Te_{11}$, and the shorter ones are for the satellites. Those at the bottom show the peak positions for $AgInTe_2$.

The atomic configuration in the AIST amorphous material, which has already been revealed by Matsunaga *et al*. [20], is heavily disordered, and has a spatially isotropic symmetry. However, it has also been revealed that it serves 3+3 coordination structures even in such a disordered atomic arrangement, as well as that of the crystalline phase: that is, both phases have similar coordination structures, i.e., locally very similar atomic arrangements (it is well known that an A7-type crystal has a 3+3 coordination structure [22], [23]). This is one of major reasons that this material achieves a sufficiently high phase-change speed by locally minimal bond interchanges. As for the dopants such as Ag or In, it has been presumed that the presence of these atoms, separately or together, serves to raise the crystallization temperature of the amorphous phase to obtain a sufficient endurance for long-term data preservation. As well as the AIST crystal, it has been revealed that GeTe or GeTe-rich GeTe-Sb_2Te_3 NaCl-type (metastable) crystals also have 3 + 3 coordination structure even in its high-temperature cubic phase [18], and that the three kinds of constituent atoms of these amorphous materials have the coordination numbers of approximately four

for Ge, three for Sb, and two or three coordination atoms for Te, fairly well satisfying the 8-N formation of Mott's rule [24]. Then, also in these amorphous materials, the average coordination number corresponds to three. These amorphous materials intrinsically contain an obvious number of crystal-like fragments in their atomic configurations [25], [26]. It is then very likely that, once sufficient energy is given to them by laser irradiation or ohmic heating, crystallization starts from these crystalline embryos all together; and whole amorphous mark are instantaneously crystallized by slight atomic shifts with bond interchanges around the embryos in the same manner of the crystal growth process revealed in AIST.

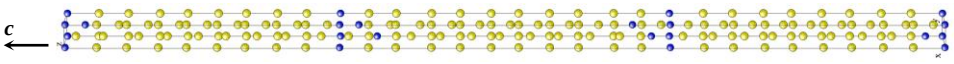

Fig. 5. Structural model of $Sb_{26}Te_3$ (820 K), which is approximated by 3D commensurately modulated structure. The atomic positions of Sb and Te are shown by yellow and blue, respectively.

4. CONCLUSION

The crystal structures of GST and AIST phase-change recording materials surprisingly resemble each other both in metastable and stable phases. However, the crystal structure in the GST materials abruptly changes with temperature from the former phase to the latter phase at first-order phase transition; on the other hand, it continuously varies in the AIST materials. This difference in transition behavior is presumed to depend on whether or not Ge atoms are present in their atomic configurations. In the amorphous phases of these materials, the atoms have three shorter and three longer coordination atoms in average. This coordination structure feature is held also in their crystalline phases. It can be considered that the structural transformation from the amorphous phase to the final (stable) crystalline phase is acquisition of anisotropic and long-range periodicities keeping the 3+3 coordination structures.

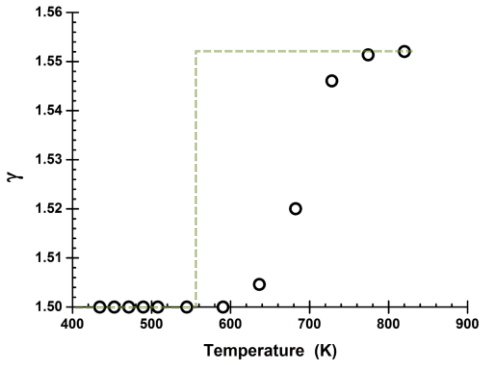

Fig. 6. Temperature dependences of modulation period (○) obtained from 4-D structural analyses for $Sb_{89}Te_{11}$. That for corresponding GST material (x=0.89) is, on the other hand, expected to vary stepwise with temperature as shown by dotted line [2].

I would like to express my sincere gratitude to Dr. A. Kolobov and Dr. P. Fons at Agency of Industrial Science and Technology for their precious advices to improve this manuscript.

REFERENCES

[1] Wuttig, M. & Yamada, N. (2007). *Nat. Mater*. **6**, 824.
[2] Yamada, N., Ohno, E., Nishiuchi, K., Akahira, N. & Takao, M. (1991). *J. Appl. Phys*. **69**(5), 1, 2849
[3] Iwasaki, H., Ide, Y., Harigaya, M., Kageyama, Y. & Fujimura, I. (1992). *Jpn. J. Appl. Phys.* **31**, 461.
[4] Nishibori, E., Takata, M., Kato, K., Sakata, M., Kubota, Y., Aoyagi, S., Kuroiwa, Y., Yamakata, M. & Ikeda, N. (2001). *Nucl. Instrum. Methods* A, **467–468**, 1045.
[5] Rietveld, H. M. *J. Appl. Cryst*. (1969). **2**, 65.
[6] Petříček, V. & Dušek, M. (2000). Jana2000 Crystallographic Computing Program, Institute of Physics, Academy of Sciences of the Czech Republic, Praha.
[7] Karpinsky, O. G., Shelimova, L. E., Kretova, M. A. & Fleurial, J. –P. (1998). *J. Alloys Compd*. **268**, 112
[8] Shelimova, L. E., Karpinskii, O. G., Zemskov, V. S., & Konstantinov, P. P. (2000) *Inorg. Mater*. **36** (3), 235.
[9] Shelimova, L. E., Karpinskii, O. G., Konstantinov, P. P., Kretova, M. A., Avilov, E. S., & Zemskov, V. S. (2001). *Inorg. Mater*. **37**(4), 342.
[10] Poudeu, P. F. P. & Kanatzidis, M. G. (2005) *Chem. Commun*. 2672.
[11] Matsunaga, T. & Yamada, N. (2004). *Phys. Rev*. B **69**(10), 104111.
[12] Matsunaga, T. & Yamada, N. Kubota, Y. (2004). *Acta Cryst.* B **60**, 685.
[13] Matsunaga, T., Kojima, R., Yamada, N., Kifune, K., Kubota, Y. & Takata, M. (2007). *Appl. Phys. Lett*. **90**, 161919.
[14] Matsunaga, T., Kojima, R., Yamada, N., Kifune, K., Kubota, Y. & Takata, M. (2007). *Acta Cryst*. B**63**, 346.
[15] Matsunaga, T., Kojima, R., Yamada, N., Kifune, K., Kubota, Y. & Takata, M. (2008). *Chem. Mater*. **20**(18), 5750.
[16] Matsunaga, T., Kojima, R., Yamada, N., Fujita, T., Kifune, K., Kubota, Y. & Takata, M. (2010). *Acta Cryst*. B**66**, 407.
[17] Lind, H. & Lidin, S. (2003). *Solid State Sci*. 5, 47.
[18] Matsunaga, T., Fons, P., Kolobov, A. V., Tominaga, J. & Yamada, N. (2011). *Appl. Phys. Lett*. **99**, 231907, 1-3
[19] Kifune, K., Fujita, T., Kubota, Y., Yamada, N. & Matsunaga, T. (2011) *Acta Cryst.* B**67**, 381.
[20] Matsunaga, T., Akola, J., Kohara, S., Honma, T., Kobayashi, K., Ikenaga, E., Jones, R. O., Yamada, N. Takata, M. & Kojima, R. *Nat. Mater*. (2011), **10**, 129.
[21] Matsunaga, T. & Yamada, N. (2004). *Jpn. J. Appl. Phys*. **43**(7B), 4704.
[22] Clark, G. L. *Applied X-Rays* (McGraw-Hill Book Company, Inc., 1955).
[23] Hoffmann, R. *Solid and Surface* (VCH, New York, 1988).
[24] Mott, N. F. (1969). *Philos. Mag.* B **19**, 835
[25] Kohara, S., Kato, K., Usuki, T., Suzuya, K., Tanaka, H., Tanaka, Y., Kimura, S., Tanaka, H., Moritomo, Y., Matsunaga, T., Yamada, N., Suematsu, H. & Takata, M. (2006). *Appl. Phys. Lett.* **89**
[26] Ohara, K., Temleitner, L., Sugimoto, K., Kohara, S., Matsunaga, T., Pusztai, L., Itou, M., Ohsumi, H., Kojima, R., Yamada, N., Usuki, T., Fujiwara, A. & Takata, M. (2012). *Adv. Funct. Matter*. **22**, 2251